Characterization of an ultrasonic flowmeter for liquid and dense phase carbon dioxide under static conditions

Yessica Arellano[1], Nicholas Mollo[2], Sigurd Weidemann Løvseth[1], Hans Georg Jacob Stang[1], Gerard Bottino[3]

***Abstract*— Carbon Capture and Storage (CCS), seen as a necessary technology to mitigate global greenhouse gas emissions, requires traceable fiscal metering technologies for large-scale deployment. The present work assesses ultrasonic measurement principles for CO_2. Static tests with pure CO_2 at pressure and temperature conditions relevant for CCS transport via ships and pipelines were undertaken; and the performance of the ultrasonic signals assessed. The effect that the CO_2 attenuation has on the signal quality is evaluated over various densities. The speed of sound measurements are presented and compared to theoretical figures. The results demonstrate that acoustic coupling efficiency of the ultrasonic wave from the transducer into the liquid is strong at high densities, but it deteriorates at transport conditions above 293 K. Consequently, measurement perspectives for shipping and pipeline conditions below 280 K show superior performance for the ultrasonic system under test. This paper also explores the limitations of ultrasonic technology for speed of sound and inter-channel variations.**

***Index Terms*— Carbon capture and storage, Carbon dioxide, Ultrasonic transducer arrays, Diagnosis, CO_2 thermodynamics**

I. Introduction

CARBON Capture and Storage (CCS) is of the upmost relevance to assist in the reduction of carbon dioxide emissions and meet climate targets [1, 2]. The IEA's sustainable development scenario [3] estimates that the annual CO_2 trade within CCS by 2050 will be 5 Gt. In Europe, the European Trading System (ETS) is an enabler of the CCS, with the associated regulations specifying accurate measurement-based methodologies to quantify the stored CO_2. The deployment of large-scale CCS will hence create a niche for flow metering not only to enable fair business and reliable custody transfer, but also for fiscal purposes. The importance of accurate measurements will grow with the expected increase in CO_2 price, which currently is above 70€ per tonne in Europe. There are, however, key challenges related to CO_2 flow metering in CCS that must be addressed [4].

Transport of large volumes of CO_2 is done via pipelines, with CO_2 being in a liquid or dense phase. At shorter distances, CO_2 may also be transported in a compressed gaseous phase. For long distances and intermediate or smaller volumes, modular transport of refrigerated liquified CO_2 by ship, train or truck could be competitive [5]. Compared with most other fluid commodities, CO_2 is in all transport modes at conditions that are in proximity to the vapor-liquid equilibrium curve, from the triple point to the critical point. The corresponding rapid changes of properties with temperature and pressure could pose specific challenges for flow metering [6-11].

However different CCS operating conditions are from those of water or natural gas transport, existing metering technologies fostered in the oil and gas industry have caught the attention for potential use within CCS. At least two benchmarking studies of flow metering technologies for application in fiscal metering for CCS have been independently conducted in recent years [12, 13]. The studies highlight the potential of Coriolis and ultrasonic methods for CCS. Verifications tests of these technologies, however, have been restricted to CO_2 and CO_2 -rich natural gas, mostly at temperatures above 288 K or liquid CO_2 or CO_2 -rich mixtures at low flow rates [14-20], with limited applicability for CCS.

The present work addresses ultrasonic flow measurements in CCS. Ultrasonic meters are non-invasive and have the potential to provide high accuracy. Further, they cause no additional pressure drop, in contrast to Coriolis and differential pressure -based technologies [12]. However, the attenuation of ultrasound waves through CO_2, dominated by the fluid's molecular thermal relaxation properties [21], has been identified as a challenge. Thermal relaxation arises due to the energy exchanged between molecular vibrations and translations. Although molecular thermal relaxation is not unique for CO_2, the predominant deterrent is that the acoustic attenuation peak for gaseous CO_2 is in the frequency range typically used in ultrasonic flowmeters, reaching attenuation coefficients up to 6 times that of natural gas at 80 kHz [16]. This effect is, however, less prominent for liquid CO_2, as the relaxation frequency is approximately proportional to density up to 900 $kg \times m^{-3}$ [22-24]. With impurities present that have faster relaxation times, the thermal relaxation frequency could also be drastically reduced, which can be leveraged in acoustic measurements [24]. Previous and ongoing research has looked into the capabilities of ultrasonic techniques for CO_2 capture and transport processes [14-16, 25]. Of particular relevance is the work in [16], where the performance of ultrasonic time-of-flight

[1] Y. Arellano S. W. Løvseth, and H. G. J. Stang are with SINTEF Energy Research, Trondheim, Norway (e-mail: yessica.arellano@sintef.no; sigurd.w.lovseth@sintef.no; jacob.stang@sintef.no).
[2] N. Mollo is with Panametrics, a Baker Hughes business, Massachusetts, USA (e-mail: nicholas.mollo@BakerHughes.com)
[3] G. Bottino is with Panametrics, a Bake Hughes business, France (e-mail: gerard.bottino@bakerhughes.com)

This is the accepted version of an article published in IEEE Sensors Journal
http://dx.doi.org/10.1109/JSEN.2022.3180075

meters with CO_2 -rich fluid was evaluated. The encouraging results of the referred work is mostly relevant for enhanced oil or gas recovery (EOR or EGR) operations or extraction of CO_2 -rich natural gas. The potential for use of ultrasonic meters for transport within CCS is yet to be independently confirmed for pure and close-to-pure CO_2. Their use in these types of applications is of interest given the ability of such meters to handle large flow rates through larger pipe sizes using a single flow meter.

The diagnostics of a time-of-flight ultrasonic flow meter unit are analysed here. The present work differs from already published research in terms of the properties of the fluid, the range of experimental conditions, and the evaluation method. Due to the lack of a traceable liquid CO_2 flow facility at relevant scale worldwide [13], the experiments were conducted under controlled static conditions. The experimental campaign looks to assess the performance of the meter at operational settings relevant for CCS shipping and pipeline transport. The evaluation method is based on enclosing liquid and dense CO_2 within a spool piece, at different pressures and temperatures, and assessing the meter diagnostics. Statistical analysis was performed on the experimental data to assess the quality of the measurements and to help understand the relationship of key variables against reference parameters. This novel approach aims to provide a better understanding of the potential use of ultrasonic meters for CCS by addressing some of the questions raised regarding the applicability of the technology for CO_2 service.

The remainder of this paper is organized into five sections as follows. Section II provides an overview of the experimental method including the setup, test matrix, and details of the ultrasonic meter under test as well as the characterization of the reference measurements. Section III discusses the experimental results and highlights of the ultrasonic meter performance. The main conclusions of this study and direction for future work is summarised in Section IV.

II. Methodology

A. Experimental setup

To explore the capabilities of ultrasonic technology for CCS, a series of experiments were conducted at the Thermal engineering laboratories of SINTEF and NTNU in Trondheim, Norway. A schematic of the experimental configuration is depicted in Fig. 1, indicating the main parts of the apparatus. The setup consists of an 8-inch (200 mm) diameter Panametrics Sentinel LCT Ultrasonic Flow meter with blind flanges bolted onto each end and an internal volume of 24 *l*. The meter was placed inside a temperature-controlled room, with temperature stability within ±1 K accuracy. The remotely mounted meter electronics, separated from the flow meter spool, were kept outside the freezing room. The meter spool was enclosed inside an insulated box for better temperature stability. The insulated box was equipped with electric heating for enhanced temperature control above 273 K. The blind flanges sealing the spool were each modified with a drilled and tapped hole in the centre to accommodate a tube for filling / emptying CO_2 in one end, and the temperature measurement probe in the opposite end. Temperature was measured 91 mm into the spool using a 100 Ω, 3-wire, stainless steel RTD probe (PR-10E-3-100-1/8-6, designated PT100) with Class A accuracy as per IEC60751, i.e., $\pm(0.015+0.02\times T)$°C.

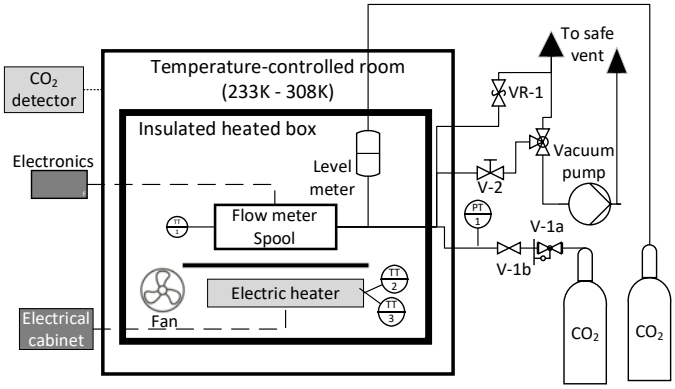

Fig. 1. Schematic of setup for experimental tests on ultrasonic flow meter.

The tube from the meter was connected to a manifold with a pressure safety relief valve, a vacuum pump, a safe vent, the feeding cylinders containing CO_2 of 99.5% purity, a pressure transmitter, and a level meter. The 200 bar (20 MPa) Keller PAA-33x pressure transmitter (PT) had a specified precision of 0.1% full scale (FS), or 0.02 MPa. The level meter, which was situated above the flow meter inside the insulated box, was installed to detect possible changes in phase.

The flow cell pressure could be logged continuously using the manufacturer's proprietary data acquisition system. The temperature and level measurement signals were acquired through a Keysight data acquisition switch unit (Agilent 34970a).

To account for a safety margin of 1.2 MPa to the setting of the pressure release valve (VR-1), the maximum operating pressure was 9 MPa.

This is the accepted version of an article published in IEEE Sensors Journal
http://dx.doi.org/10.1109/JSEN.2022.3180075

B. Experimental procedures

Before CO_2 was fed into the system, with the setup at ambient temperature, all gas from within the setup was evacuated, after which valve V2 was closed. As the freezing room reached the desired temperature, the meter was charged by opening valves V1a and V1b. When the fluid temperature had stabilized and the desired pressure was reached, valves V1a and V1b were closed before starting the measurements.

Measurements were acquired in decreasing order of density (see Fig. 2). In general, that meant starting at the lowest temperature and at the highest pressure for that temperature setting. To release pressure from the spool, either at the same temperature, or if needed when going to the next higher temperature, valve V2 was opened slightly while V1b remained closed, flushing the line from the meter body in the process. If needed, injecting more fluid into the setup was still possible at pressures below 5.7 MPa (pressure of the feeding cylinder).

Care was taken when selecting experimental points close to the saturation curve to avoid gasification of the fluid. A margin of at least 0.07 MPa was used for all temperature points. If a phase change was detected, for instance from the level meter, actions were taken to ensure the fluid in the flow meter cell was always in the liquid state. All experiments were conducted at controlled temperature conditions. Data was gathered for at least 5 min for every test point.

The primary concern of the study is the performance of the meter given the acoustic characteristics of CO_2; where the attenuation coefficient and speed of sound are theoretically known and can be computed from Lin and Trusler model [24] and Span-Wagner equation of state (EOS) [26], respectively. However, as discussed below, our attempts to replicate these were only partially successful.

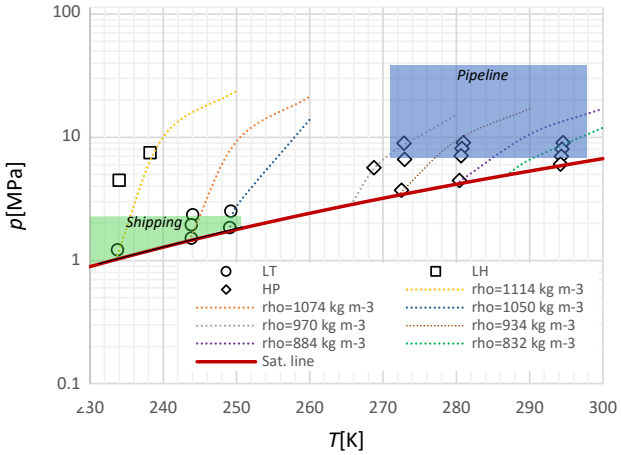

Fig. 2. Experimental matrix showing high-pressure (HP) points in diamonds, low-temperature (LT) in circles, and low-temperature/high-pressure (LH) in squares, along with the CO_2 gas-liquid saturation curve, isochoric curves, and exemplary conditions relevant for pipeline and ship transport of CO_2 in CCS.

C. Experimental matrix

The fluid test condition and property ranges are summarised in TABLE I. The experimental matrix was designed to cover fluid properties typical to both shipping and pipeline transport conditions for CCS. Data were collected at 20 different fluid conditions: Six low-temperature (LT) test points, ran at pressures above the saturation curve for temperatures of 234 K, 244 K, and 249 K (see TABLE II), and twelve high-pressure (HP) test points at pressures up to 9 MPa and temperatures between 269 K and 294 K (see TABLE III); two additional test points to cover the lower end of the operational envelope of the experimental setup, combining low-temperature and high-pressure conditions (designated LH in TABLE IV) were also gathered.

TABLE I
EXPERIMENTAL TEST CONDITIONS AND FLUID PROPERTIES.

Pressure [MPa]	1.5 – 9.0 (±0.02)
Temperature [K]	233 – 293 (±1)
Density [kg×m^{-3}]	760 – 1125
Speed of Sound [m×s^{-1}]	330 – 875
Phase	Liquid / Dense

TABLE II.
LOW-TEMPERATURE (LT) TEST POINTS.

Test Point	Setpoint temperature [K]	Setpoint pressure [MPa]	Measured temperature [K]	Measured pressure [MPa]	Density [kg×m^{-3}]
LT-1	249	2.5	249.242	2.516	1052.5
LT-2	249	1.9	249.094	1.855	1050.5
LT-3	244	2.4	244.032	2.359	1075.2
LT-4	244	2.0	243.860	1.956	1074.5
LT-5	244	1.5	243.831	1.519	1073.1
LT-6	234	1.2	233.765	1.222	1114.6

TABLE III.
HIGH-PRESSURE (HP) TEST POINTS.

Point	Setpoint temperature [K]	Setpoint pressure [MPa]	Measured temperature [K]	Measured pressure [MPa]	Density [kg×m^{-3}]
HP-1	269	5.7	268.760	5.6767	970.92
HP-2	273	8.9	272.879	8.9334	969.17
HP-3	273	6.6	272.946	6.636	953.95
HP-4	273	3.7	272.546	3.725	933.68
HP-5	281	9.0	280.947	9.028	925.58
HP-6	281	8.1	280.794	8.102	918.93
HP-7	281	7.1	280.680	7.097	910.73
HP-8	281	4.5	280.438	4.467	883.99
HP-9	295	9.0	294.575	9.037	832.18
HP-10	295	8.0	294.431	8.041	816.66
HP-11	295	7.0	294.333	7.008	795.72
HP-12	295	6.0	294.217	6.055	768.79

TABLE IV.
LOW-TEMPERATURE AND HIGH-PRESSURE (LH) TEST POINTS.

Test Point	Setpoint temperature [K]	Setpoint pressure [MPa]	Measured temperature [K]	Measured pressure [MPa]	Density [kg×m^{-3}]
LH-1	234	4.5	234.016	4.4778	1122.7
LH-2	238	7.5	238.220	7.489	1114.8

This is the accepted version of an article published in IEEE Sensors Journal
http://dx.doi.org/10.1109/JSEN.2022.3180075

D. Characterisation of reference measurements

Reference measurements for pressure and temperature were characterized. The initial examination consisted of setting up a target temperature of 278.65 K (5.5°C) in the control system of the freezing room and 280.15 K (7°C) in the insulated box. Once the temperature inside the spool had reached stable conditions, the temperature signal was monitored over a 120 min period, i.e., 15 times the measurement windows (5 min) for every test point in the experimental campaign (see Fig. 3a). This period is sufficient to characterise the temperature measurement; given how short the measurement window is for every experimental point, no long-term temperature drift was assessed. The measured temperature, sampled every second, averaged around 280.437 K with a variation within a 0.011 K interval and standard deviation of 0.002 K, well within the accuracy limits of the PT100 at the given operating range (±0.155 K). A similar, yet shorter, test of 20 min was conducted at a lower temperature target of 250.15 K (-23°C). In this case, as for all test points below 273 K, the heating system inside the insulation box was disabled to ease temperature control, hence leaving the temperature control to the freezing room system. The maximum temperature measurement variation was still within an acceptable interval of 0.085 K and had a standard deviation of 0.008 K, while the accuracy of the PT100 at the given temperature was ±0.475 K.

The pressure measurements for the same 120-minute period in Fig. 3a averaged 4.64 MPa ±0.035 MPa SD. The variation is

larger than the accuracy of the pressure sensor (±0.02 MPa), hence indicating the deviation responds to an actual physical phenomenon, which is supported by the correlation between temperature and pressure variations plotted in Fig. 3b.

The temperature and pressure variations reported above correspond to estimated changes in the fluid sound speed of up to 0.286 $m \times s^{-1}$ or 0.06% of the theoretical speed at the setup conditions, calculated using the Span-Wagner EOS [26]. Any deviations in the measured speed of sound, from theoretical values, below 0.06% can be attributed to the setup uncertainty.

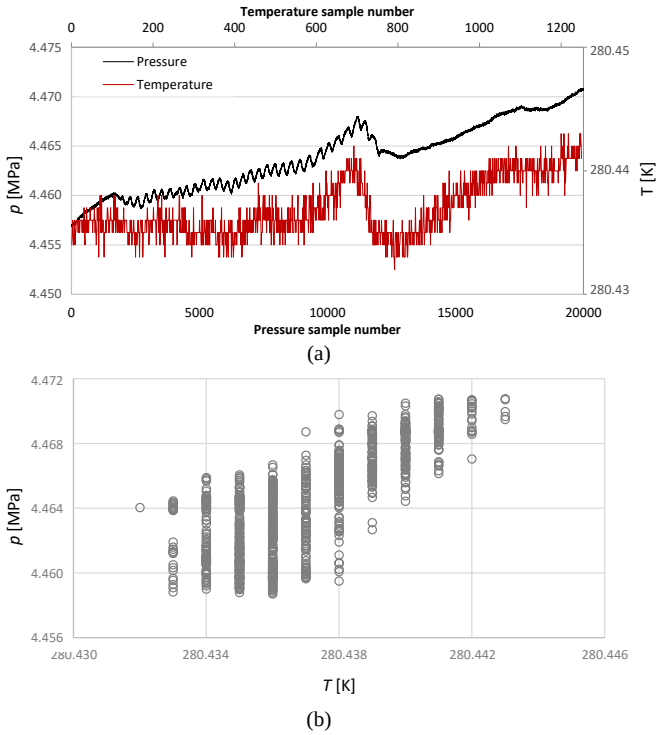

Fig. 3. Reference signal monitoring showing (a) temperature and pressure drift over a 120 min period and (b) measured pressure as a function of measured temperature

E. Ultrasonic measurements

The ultrasonic meter used in this test utilizes multiple measurement paths through the measurement volume. Fig. 4 shows a simplified cutaway of a single path, ultrasonic flow meter where L_{path} is the path length across the pipe and through the fluid that the ultrasonic signal passes, Q is the angle between the pipe centreline and the transducer path, and t_{up} and t_{dn} are the upstream and downstream transit times taken by the ultrasonic signal to pass through the fluid. The time it takes the signal to travel through the fluid in the upstream and downstream directions is different when the fluid is flowing, and this is how the meter normally calculates the volumetric flow rate. For this entire test series, the liquid/dense phase CO_2 fluid was always static, with the exception of any internal convective currents that may have arisen within the enclosed volume. The speed of sound measurement is a direct result of time-based calculations of the signal processing and the geometric parameters of the flow cell.

The transducer frequency of the meter used for this test was 500 kHz. The meter under test consisted of a 4-path chordal configuration with two orthogonal measurement planes. With the meter positioned horizontally, paths, or channels (Ch), 1 and 4 correspond to the outermost transducers, near the top and bottom of the meter body, respectively. The innermost transducers, with the longer path length, are referred in the following as Ch2 and Ch3. Each of the two pairs of perpendicular, crisscrossing paths are at the same radial distance from the pipe centerline and are symmetrical about the axial center line of the pipe from top to

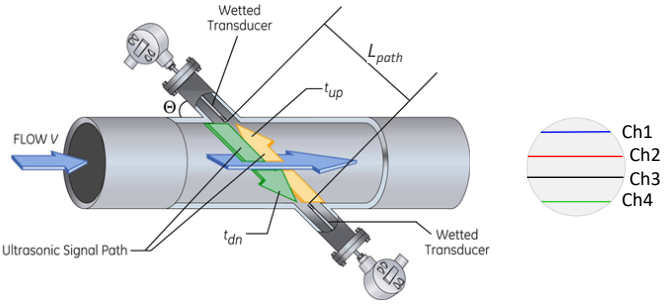

Fig. 4. Simplified cutaway of (a) a single path, ultrasonic flow meter showing the path length (L_{path}) and the upstream and downstream transit times, tup and tdn, respectively, and (b) cross-section view of the position of the channels 1 to 4.

This is the accepted version of an article published in IEEE Sensors Journal
http://dx.doi.org/10.1109/JSEN.2022.3180075

bottom of the pipe.

The real time diagnostic data from the ultrasonic meter was acquired via the meter manufacturer's data logging and display software which included capabilities such as historical tracking of diagnostics and a full configuration audit trail. The main parameters monitored and logged during each test point were individual channel flow velocities, up and down transit times, speed of sound measurements, signal to noise ratio, and other receiver diagnostics for further inter-channel variance assessment.

F. Estimation of the sound attenuation coefficient of liquid CO_2

One of the most relevant question marks relating to ultrasonic meter performance is sound attenuation through CO_2, associated with a long vibrational relaxation time. Although sound attenuation in liquid or supercritical CO_2 is lower than for the gas phase [22], it has implications in the ultrasound signals and hence needs a close assessment. The acoustic attenuation was computed similarly to Lin and Trusler [24] for CO_2 in liquid and supercritical states. The present work estimates the vibrational relaxation time of pure CO_2 [27] as proposed by Deng et al. [28], i.e. considering the CO_2 characteristic temperature of different vibrational modes.

Acoustic attenuation in general decreases with density in the investigated domain (see Fig. 5), mainly driven by the increase in molecular thermal relaxation frequency. The absorption coefficient α for the test conditions in the present work, based on models in [24] and [28], is shown in Fig. 6. The trends are consistent with Lin and Trusler predictions for higher pressure and temperature ranges.

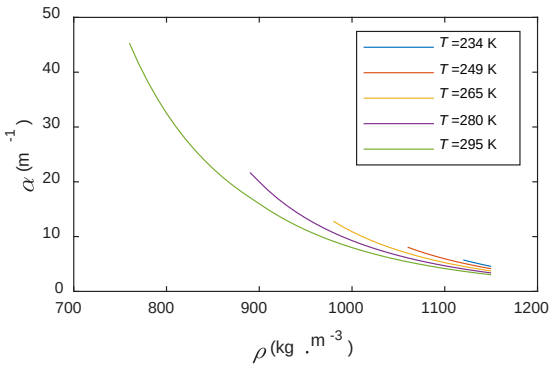

Fig. 5. Theoretical attenuation of CO_2 at an acoustic frequency 500 kHz as a function of density based on the model of [24, 28].

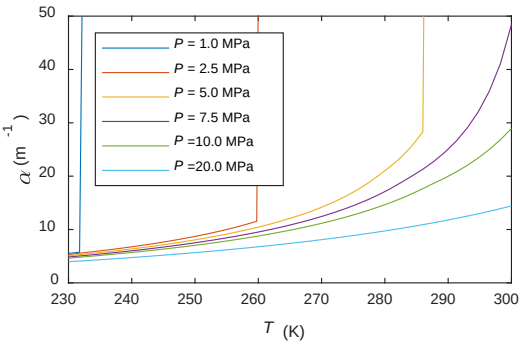

Fig. 6. Ultrasonic absorption coefficient of liquid CO_2 at 500 kHz computed from [24] and [28]

III. Results and Discussion

A. Performance

The performance of the ultrasonic meter was assessed by monitoring the following four parameters.

1) *Gain*

The meter electronics work to keep the received signal voltage at a constant level via an automatic gain control circuit. Gain is an indication of the acoustic signal strength. Fig. 7 shows the amplitude gain of all paths for all 20 test points. An early observation is that the signal from transmission to receiver transducer in dense/liquid CO_2 is less attenuated when the fluid is colder, and the density is higher.

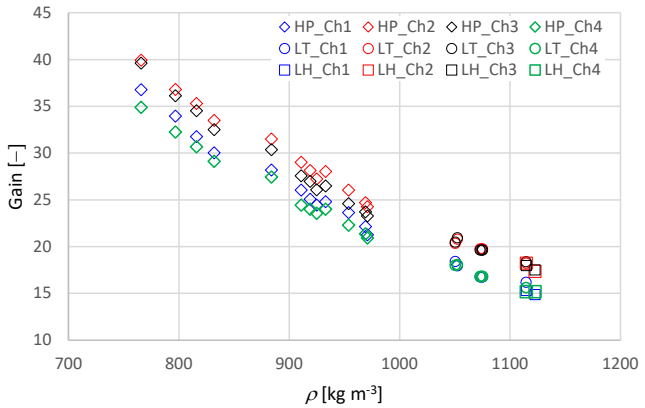

Fig. 7. Density vs. amplitude gain of all four channels (Ch1-blue, Ch2-red, Ch3-black, and Ch4-green) and the different groups of test points defined in Tables II – IV (high pressure (HP) test points in diamonds, low temperature (LT) in circles and low-temperature/high-pressure (HL) in squares).

The gain levels of the outer paths, Ch1 and Ch4, are seen to be lower than the gain for the inner paths, Ch2 and Ch3. This is consistent with the longer path lengths between the outer compared to the inner transducer pairs, resulting in larger acoustic attenuation in the former.

The continuous gain increase with decreasing density is related to two factors. Firstly, increased fluid density with a better matched acoustic impedance with the transducer results in higher energy permeation, which translates to stronger signals and lower needed receiver gains [29]. As the acoustic impedance of the fluid further deviates from that of the sensor, less of the wave is "absorbed" into the transducer. Weaker received signals force an increase in the automatic gain controller, therefore higher gain values. Secondly, acoustic attenuation, which is mainly driven by the increase in molecular thermal relaxation frequency, decreases with increasing density as we know from theory (see Fig. 5).

This is the accepted version of an article published in IEEE Sensors Journal
http://dx.doi.org/10.1109/JSEN.2022.3180075

Whereas the overall trend in Fig. 7 is clear, it can also be observed that gains between symmetrical paths (Ch1/Ch4 and Ch2/Ch3) begin to diverge for the higher temperature points, below the fluid density of 1000 kg×m^{-3}. The signal noise increases with decreasing density, as will be discussed further, and even relatively small differences in signal quality will be apparently larger from channel to channel, forcing the gain controller to react differently, even for symmetrical paths.

Fig. 8 shows the relation between the signal strength and the sound attenuation of the CO_2. Fig. 8b illustrates the surplus attenuation, which could theoretically be attributed to the impedance mismatch.

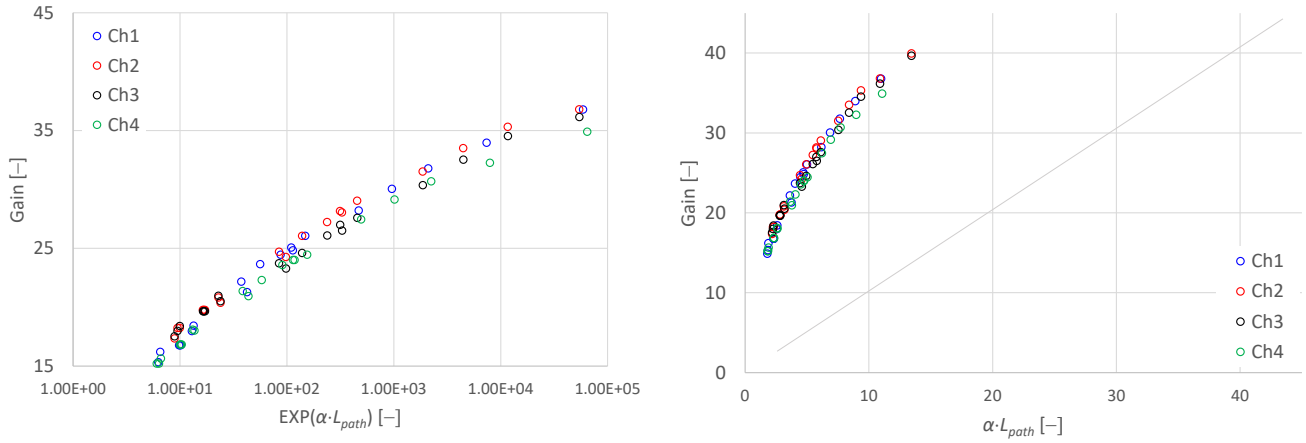

(a) (b)

Fig. 8. Gain increase with (a) signal attenuation as an exponential function of the path length through the medium attenuation and (b) attenuation coefficient of all paths for all data points

2) *Signal-to-Noise Ratio (SNR)*

The SNR is another indication of the signal quality. The performance of the meter could be impaired if the transducers receive background acoustic noise from extraneous sources. SNR is expected to be an issue, even at static conditions, when the fluid is extremely attenuative, in which case, regardless of how much gain is applied, all that is picked up by a receiving transducer is noise. SNR was monitored across all test points as a health indicator in the present test campaign and will be used as baseline in future flow tests as well. Fig. 9 shows the range of the SNR measured among all four channels for all data points plotted in order of increasing temperature. Similar to the gain data, the SNR values show a decreasing signal quality with increasing temperature and decreasing density. The SNR for the measurement points at temperatures below 249 K were consistently above 20, with a maximum registered of 83.2. The SNR for the high-pressure (HP) data shows lower figures, with sustained measurements with SNR below 20 for temperatures of 281 K and above.

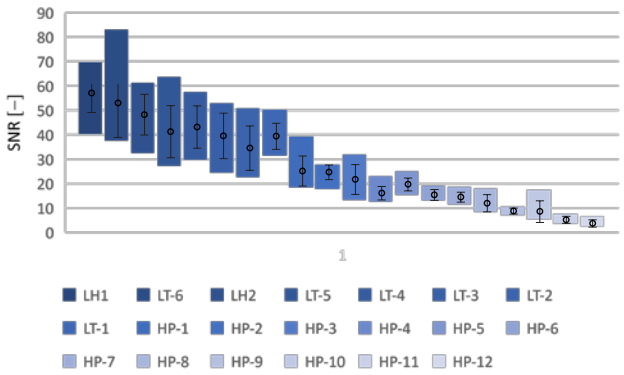

Fig. 9. Range of signal-to-noise (SNR) measured shown as blue bars for all test points. Mean SNR is indicated by circles and standard deviation by error bars. The data include all channels and is presented in increasing temperature order.

Various factors can decrease the SNR of the acoustic signals across the flow meters. The presence of gas bubbles, or non-homogenous mixing of two liquids in a liquid meter will cause low SNR. In the present case, after ruling out gasification of the fluid within the spool, signal attenuation and impedance matching factors are the alternative source of the evidenced signal degradation.

For selected measurements, the raw transducer signals were monitored and recorded. Fig. 10 compares the raw signals from the transducers on Ch3, with (a) being the base case with SNR equal to 51.2 during a static water calibration at the Panametrics factory prior to the test, (b) an SNR of 45.9 during test point LH-2, and (c) one of the lowest registered SNR values of 8.1 in the present CO_2 experiments at test point HP-9. Received signals are cleaner and more pronounced at higher density.

This is the accepted version of an article published in IEEE Sensors Journal
http://dx.doi.org/10.1109/JSEN.2022.3180075

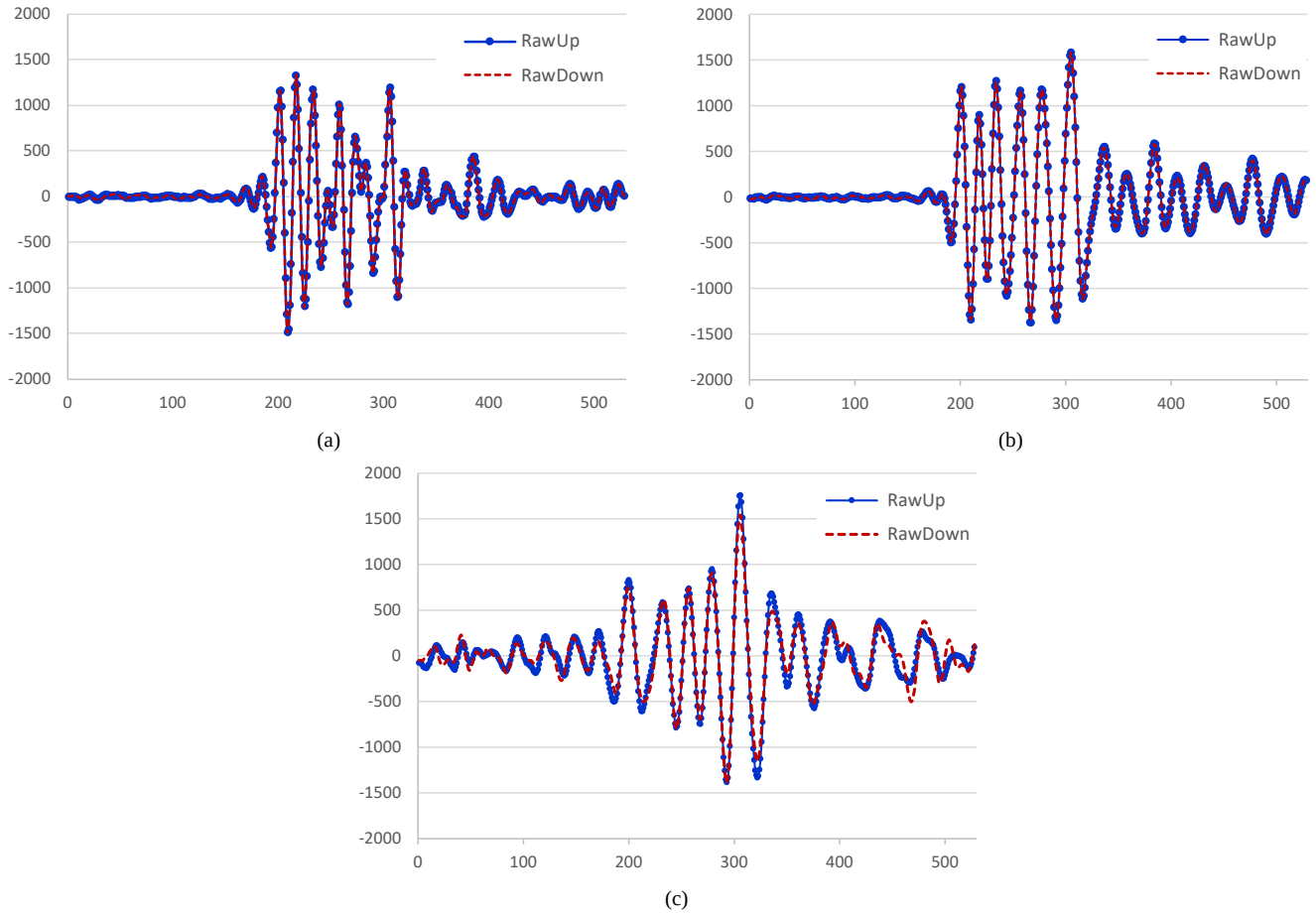

Fig. 10. Channel 3 Raw signals from transducers showing upstream and downstream through transmission signals from (a) static water calibration SNR of 51.2, (b) test point LH-2 SNR of 45.9, and (c) test point HP-9 with SNR of 8.1.

3) *Inter-channel variance*

The measurement principle of transit time ultrasonic flow meters is based on the concept that the difference between the upstream and downstream signal transit times, D*t*, is directly proportional to the flow velocity [30]. Under no-flow conditions, theoretically, D*t* should tend to zero.

Fig. 11 shows the combined ranges of the measured transit time differences for all channels for every test point. The intrinsic variation in signal transit times due to different lengths among the paths is also contained within the reported ranges.

The absolute value of the average time differences per channel is below 4 ns for the low-temperature points and below 10 ns for most high-pressure points, except for HP-11 and HP-12 where the average D*t* was -30 ns and 27 ns, respectively. The cause of these evident increase is the degradation in signal quality as the CO_2 density – and speed of sound – decreased considerably from the low temperature points, leading to an increase in attenuation and larger impedance mismatch, as discussed above.

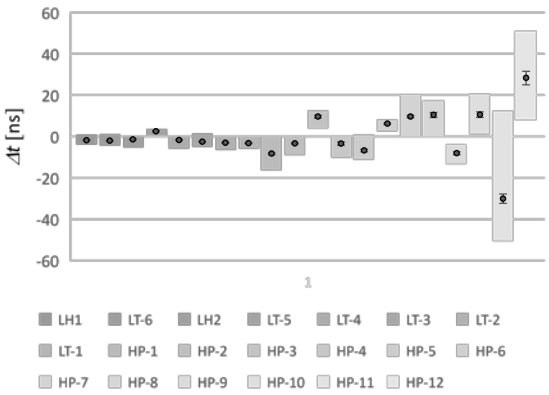

Fig. 11. Ranges of transit time differences (D*t*) shown as grey bars for all test points. Mean transit times are shown using circles and standard deviation using error bars. The ranges include all channels and are presented in increasing temperature order of the associated data points.

Comparing the signal from the base case (water) and LH-2 in Fig. 10 (a) and (b), respectively, against the test points of varying density in Fig. 12, i.e., LT-1, HP-2, HP-7, and HP-12, the change in signal shape to the point of nearly-no-clear signal in Fig. 12 (d) with the lowest density, is clear. When the signal amplitude falls to that of the noise, the ability of the meter to process the signals is diminished and the resulting measurements can be incorrect.

While this behavior may seem detrimental to using ultrasonic flow meters for pipeline transport measurements, there are other techniques that could be implemented to better compensate for the reduced signal quality of the lower fluid densities. These

This is the accepted version of an article published in IEEE Sensors Journal
http://dx.doi.org/10.1109/JSEN.2022.3180075

options may be explored in possible future tests.

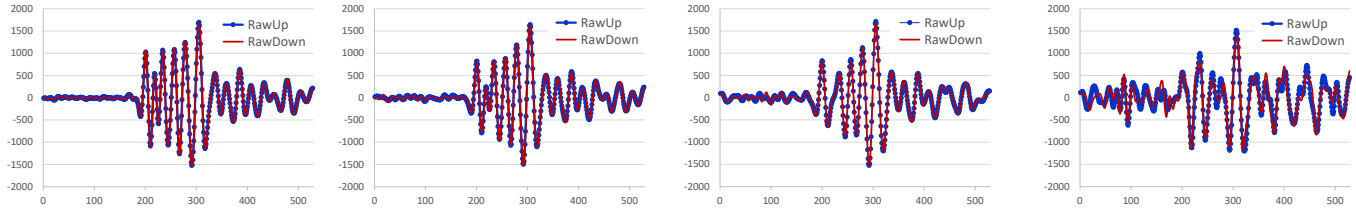

Fig. 12. Channel 1 Raw signals from transducers showing upstream and downstream through transmission signals for (a) LT1, (b) HP2, (c) HP7, and (d) HP12.

4) *Speed of Sound*

Fig. 13 shows the measured speed of sound (*c*) for all test points contrasted against theoretical values from Wagner-Span EOS [26]. Span-Wagner EOS was derived based on existing datasets that encompass the conditions of the current test matrix, i.e. Novikov and Trenlin at 288-373 K 3-10 MPa. Reportedly, although no reasonable uncertainty estimation of the above-mentioned dataset is provided, the overall uncertainty of the Span-Wagner model for speed of sound calculations in the region of interest is expectedly ±0.5% to ±1.0%. The measured and calculated speed of sound show the same trend of decreasing speed with decreasing density, i.e., increasing temperature and decreasing pressure. The measured data are consistently higher than the model estimates, with deviations up to 3% for temperatures below 273 K and increasing deviations for lower densities, up to 12.8% for HP-12 at 294 K as seen in the inner graph therein.

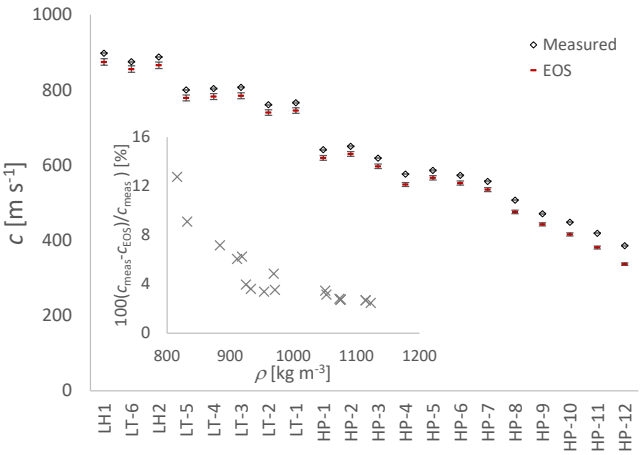

Fig. 13. Measured and theoretical speed of sound (*c*). The mean speed of sound for all measurement channels are shown using diamonds and standard deviation of the measurements using error bars. The Span-Wagner EOS [26] is used to calculate the theoretical values, and its reported model accuracy as error bars for all test points. The data are arranged in increasing temperature order. The inner graph shows the percentage deviation of speed of sound (*c*) measurements from Span-Wagner EOS for different densities.

Several factors can contribute to the deviations between the theoretical sound speed and the meter measurements. Firstly, an error in the water temperature measurement during static calibration of the meter could yield deviations in the speed of sound measurements, yet such error should expectedly account for less than one percent and be somewhat consistent throughout the tests. Secondly, signal distortion, as per the signal quality reviewed above, shows dramatic changes across the density range, which is likely to play a larger role in the measurement errors noted. Thirdly, signal processing algorithms can be potentially locking onto an echo rather than the main through transmission signal, yet the data collected at the time of the test is insufficient to confirm this hypothesis.

IV. Conclusions

The acoustic signal quality from a multi-path ultrasonic flow meter transducers transmitting through dense/liquid CO_2 at 20 temperature and pressure conditions was evaluated using a specially built test setup. The main contribution of this work is the demonstration that ultrasonic meters have a real potential for measurement of liquid CO_2 streams.

Changes in the fluid density at different testing conditions lead to a change of the acoustic coupling efficiency of the ultrasonic wave from the transducers into the CO_2. Higher densities result in higher acoustic impedance and better coupling which yields higher signal quality.

Estimations of the absorption coefficient illustrate that vibrational relaxation at the operational frequencies of 500 kHz, will keep sound absorption at a level at which measurements of the speed of sound are possible. For most high pressure/high temperature points, the ultrasonic signals were still strong enough to traverse through the fluid enabling measurement of relevant data by the meter. There was signal degradation at the lowest densities, and the speed of sound measurements show a significant reduction in accuracy and stability for temperatures above 293 K, relevant for onshore CCS pipeline transport. The new knowledge represents another contribution of the work, as it challenges the idea that water calibration is sufficient prior to deployment of metering units in the field. The settings of the meter need to be optimized for CCS applications. Further work shall be undertaken to assess alternative techniques to compensate for the reduced signal quality of the lower fluid densities, relevant for CCS pipeline transport.

Ensuring the signal being processed is the actual acoustic signal and not just noise, is important. Looking at the raw transducer signals, the signal peaks of the acoustic signal is still apparent, even as the surrounding noise increases at low CO_2 densities. Diagnostic logs can also be reviewed for errors, warnings, and other signs which would indicate problems with the signal processing. Issues did arise during the data points taken on the less dense fluid. Future tests will be performed targeting extended experimental conditions around those where issues were evidenced followed by a closer observation of the raw signals. Also,

This is the accepted version of an article published in IEEE Sensors Journal
http://dx.doi.org/10.1109/JSEN.2022.3180075

future tests could find more optimal ways of processing the weaker signals encountered in what is considered relevant conditions of pipeline transport for CCS.

This study, limited to static conditions, precludes the evaluation of dynamic effects that are known to influence the performance and accuracy of ultrasonic flow meters, such as velocity profile and turbulence.

ACKNOWLEDGMENT

This publication has been produced with support from Panametrics, a Baker Hughes business, and the NCCS Centre, performed under the Norwegian research program Centers for Environment-friendly Energy Research (FME). The authors acknowledge the following partners for their contributions: Aker Carbon Capture, Allton, Ansaldo Energia, Baker Hughes, CoorsTek Membrane Sciences, Equinor, Fortum Oslo Varme, Gassco, KROHNE, Larvik Shipping, Lundin Norway, Norcem, Norwegian Oil and Gas, Quad Geometrics, Stratum Reservoir, Total, Vår Energi, Wintershall DEA and the Research Council of Norway (257579/E20)

REFERENCES

[1] "Energy Technology Perspectives 2017," International Energy Agency, Paris, France, http://www.iea.org/etp/, 2017.
[2] V. Masson-Delmotte et al., Eds. Global Warming of 1.5°C. https://www.ipcc.ch/sr15/: IPCC, 2018.
[3] "World Energy Outlook 2020," International Energy Agency, Paris, France, 2020. [Online]. Available: https://www.iea.org/weo
[4] A. M. Moe et al., "A Trans-European CO2 Transportation Infrastructure for CCUS: Opportunities & Challenges," Advisory Council of the European ZeroEmission Technology and Innovation Platform (ETIP ZEP), https://zeroemissionsplatform.eu/a-trans-european-co2-transportation-infrastructure-for-ccus-opportunities-challenges/, 2020.
[5] COMMISSION DELEGATED REGULATION (EU) 2020/389 amending Regulation (EU) No 347/2013 of the European Parliament and of the Council as regards the Union list of projects of common interest, T. E. Commission, 2019.
[6] C. Mills, "Flow Measurement in support of Carbon Capture, utilisation and Storage (CCUS)," TUV SUD NEL, 2021, vol. 2021_299. [Online]. Available:https://www.instmc.org/Portals/0/SIG%20Repositories/Flow%20Measurement%20SIG/Flow%20Measurement%20in%20Support%20of%20CCUS.pdf
[7] G. FitzGerald, "Cork CCS Project Overview," in UKCCSRC Network Conference, Cardiff, 2019.
[8] Acorn, "Project: ACT Acorn Feasibility Study - Final Report," 2019. [Online]. Available: https://actacorn.eu/sites/default/files/ACT%20Acorn%20Final%20Report.pdf
[9] Rotterdam CCUS. "Project Porthos: CO2 transport and storage." https://www.porthosco2.nl/wp-content/uploads/2020/04/January-2020-handout-Porthos-ENG.pdf
[10] Northern Lights. "Accelerating decarbonisation." https://northernlightsccs.com/.
[11] ATHOS. "The Athos project." https://athosccus.nl/project-en/
[12] S. W. Løvseth, Y. Arellano, H. Deng, F. Finotti, E. Jukes, and G. Bottino, "Enabling CCS via Fiscal Metering," presented at the Trondheim CCS 11 Proceedings, , Trondheim, 2021. [Online]. Available: https://www.sintef.no/globalassets/project/tccs-11/tccs-11/sproceedings-no-7.pdf.
[13] J. M. Kocbach, *et al*, "Where do we stand on flow metering for CO2 handling and storage?," presented at the *38th International North Sea Flow Measurement Workshop*, Aberdeen, UK, Oct, 2020.
[14] D. Van Putten and R. Kruithof, "Flow meter performance under CO2 gaseous conditions," presented at the *39th North Sea Flow Measurement Worshop*, Tønsberg, Norway, 2021.
[15] J. Wenzel, "Evaluations on CO2 Rich Natural Gas," presented at the *European Flow Measurement Workshop* 2015, Noordwijk, 2015. [Online]. Available: https://sportdocbox.com/Scuba_Diving/100525697-Evaluations-on-co2-rich-natural-gas-jorg-wenzel-sick.html.
[16] K. Harper and T. Dietz, "Field Experience of Ultrasonic Flow Meter Use in CO2-Rich Applications," in *27th North Sea Flow Measurement Workshop*, Tønsberg, Norway 2009
[17] C.-W. Lin, M. Nazeri, A. Bhattacharji, G. Spicer, and M. M. Maroto-Valer, "Apparatus and method for calibrating a Coriolis mass flow meter for carbon dioxide at pressure and temperature conditions represented to CCS pipeline operations," *Applied Energy*, vol. 165, pp. 759-764, 2016.
[18] L. Sun, Y. Yan, T. Wang, X. Feng, and P. Li, "Development of a CO2 two-phase flow rig for flowmeters calibration under CCS conditions," presented at the *FLOMEKO*, Sydney, Australia, 2016.
[19] L. Wang, J. Liu, Y. Yan, X. Wang, and T. Wang, "Mass flow measurement of two-phase carbon dioxide using Coriolis flowmeters," in *2017 IEEE International Instrumentation and Measurement Technology Conference (I2MTC)*, 2017: IEEE, pp. 1-5.
[20] J. Mahmoud Nazeri and Mercedes Maroto-Valer and Edward, "The Fiscal Metering of Transported CO2-Rich Mixtures in CCS Operations," *Energy Procedia*, vol. 114, pp. 6766-6777, 2017, DOI: 10.1016/j.egypro.2017.03.1808.
[21] R. W. Leonard, "The Absorption of Sound in Carbon Dioxide," *Journal of the Acoustical Society of America*, vol. 12, pp. 241-244, 1940, DOI: 10.1121/1.1916097.
[22] H. Hollander, E. Jukes, S. W. Løvseth, and Y. Arellano, "The challenges of designing a custody transfer metering system for CO2" presented at *39th North Seas Flow Measurment Workshop*, Tønsberg, Norway, 2021.
[23] P. Giustetto et al., "Heat Enhances Gas Delivery and Acoustic Attenuation in CO2 Filled Microbubbles," in *30th Annual International Conference of the IEEE Engineering in Medicine and Biology Society*, 2008, pp. 2306-2309, DOI: 10.1109/IEMBS.2008.4649659.
[24] C.-W. Lin and J. P. M. Trusler, "Speed of Sound in (Carbon Dioxide + Propane) and Derived Sound Speed of Pure Carbon Dioxide at Temperatures between (248 and 373) K and at Pressures up to 200 MPa," *Journal of Chemical & Engineering Data* vol. 50, 12, pp. 4099-4109, 2014, DOI: 10.1021/je5007407.
[25] P. Koulountzios, S. Aghajanian, T. Rymarczyk, T. Koiranen, and M. Soleimani, "An Ultrasound Tomography Method for Monitoring CO2 Capture Process Involving Stirring and CaCO3 Precipitation," *Sensors*, vol. 21, no. 21, p. 6995, 2021. [Online]. Available: https://www.mdpi.com/1424-8220/21/21/6995.
[26] R. Span and W. Wagner, "A New Equation of State for Carbon Dioxide Covering the Fluid Region from the Triple-Point Temperature to 1100 K at Pressures up to 800 MPa," *J. Phys. Chem. Data*, vol. 25, 6, 1996.
[27] K. Johnson, "Fundamentals of Thermodynamics (Lecture 16)," University of Pittsburgh, 2013.
[28] H. Deng, S. W. Løvseth, and E. Jukes, "Benchmarking and a test plan for verification of selected relevant technologies for fiscal metering in CCS," NCCS, Trondheim, Norway, Tech. Memo. DT8_2018_5, Nov 16, 2018.
[29] A. S. Dukhin and P. J. Goetz, "Fundamentals of Acoustics in Homogeneous Liquids: Longitudinal Rheology," in *Studies in Interface Science*, vol. 24: Elsevier, 2010, pp. 91-125.
[30] L. Li et al., "Experimental and Numerical Analysis of a Novel Flow Conditioner for Accuracy Improvement of Ultrasonic Gas Flowmeters," *IEEE Sensors Journal*, 2022.

This is the accepted version of an article published in IEEE Sensors Journal
http://dx.doi.org/10.1109/JSEN.2022.3180075

Yessica Arellano received her BE and M.Sc. degrees from La Universidad del Zulia, Venezuela. A second M.Sc. with distinction was awarded by the Robert Gordon University, UK. Her doctoral research at Coventry University, UK (2020), focused on advanced multiphase flow monitoring through electromagnetic measurements. For 11 years, she worked within the Oil and Gas Industry, initially in offshore facilities and later as a R&D Engineer at INTEVEP S.A. She has provided consultancy services for technology development and holds inventorship of two patents of multiphase flow metering technologies. Currently, she is a Research Scientist in SINTEF Energi AS, with a main research focus flow measurement related to CCS.

Nicholas J. Mollo received his B.S. degree in Mechanical Engineering from Worcester Polytechnic Institute, Massachusetts, USA in 1995 and his Master's degree in Mechanical Engineering from Rensselaer, New York, USA in 1998. Nick is a Principal Engineer of Flow Metrology has been with Panametrics, a Baker Hughes business, located in Billerica, Massachusetts, USA since 2018 and he has been with the company since 2003. His main focus has been on the company's custody transfer line of liquid ultrasonic flow meters and their applications outside of typical hydrocarbon markets. Prior to his work with Panametrics, he was a Lead Test Engineer with the GE Energy Steam Turbine Aerodynamics department.

Sigurd Weidemann Løvseth received his Siv.Ing. degree in physics from the Norwegian Institute of Technology, University of Trondheim, Norway in 1996. Løvseth received his Dr. Ing. degree on fiber optic sensors and lasers in 2001 at the Norwegian University of Science and Technology, also in Trondheim, Norway, earning him the Young Researcher Prize 2003 of the Royal Norwegian Society of Sciences and Letters. For 9 years, he worked in the industry and in the Norwegian Defence Research Establishment on development of fiber optic sensor systems for oil and gas and naval applications. He is a Senior Research Scientist of SINTEF Energy Research (SER), where he has been since 2009, with a main research focus on thermophysical properties of fluids and fiscal metering related to CCS. He has managed the design and construction of multiple advanced experimental facilities and led a number of research projects. Løvseth has been visiting researcher at CERN, University of Minnesota, University of Sydney, and University of Western Australia, and he has co-authored four patents.

Jacob Stang received his M.Sc degree from the Norwegian University of Science and Technology, Trondheim, Norway. His doctoral research from the same University, focused on Modelling and simulation of Flowmeter Installation Effects. Currently he is working as a research scientist at SINTEF Energy.

G. Bottino received his M.Sc. degree in Technology and Sales of Scientific Apparatus from Marseille University (France) in 1988. Gerard is the Global Commercial Development and Technical Support with Panametrics, a Baker Hughes business since 2020 and has been with the company since 2008. His area of expertise covers flow measurement with a special focus on ultrasonic transit time technology. Prior to Panametrics, Gerard worked for different companies in the field of instrumentation and process equipment for the energy industry where he held various roles over his 32 years of experience.

This is the accepted version of an article published in IEEE Sensors Journal
http://dx.doi.org/10.1109/JSEN.2022.3180075